

1 **Structural Vibration Serviceability: New Design Framework**
2 **Featuring Human-Structure Interaction**

3
4
5

6 **Erfan Shahabpoor^a, Aleksandar Pavic^{b,c}, Vitomir Racic^{d,e}**

7
8 ^a INSIGNEO Institute for In-silico Medicine, The University of Sheffield,
9 Department of Civil & Structural Engineering, Sir Frederick Mappin Building,
10 Mappin Street, Sheffield, S1 3JD, UK.

11 ^b College of Engineering, Mathematics and Physical Sciences, Vibration
12 Engineering Section, University of Exeter, North Park Road, Exeter EX4 4QF, UK.

13 ^c Full-scale Dynamics, Ltd. Kay Building, North Park Road, Exeter EX4 4QF, UK.

14 ^d Department of Civil and Environmental Engineering, Politecnico di Milano,
15 Piazza di Leonardo Da Vinci 32, Milano 20133, Italy.

16 ^e Department of Civil & Structural Engineering, The University of Sheffield, Sir
17 Frederick Mappin Building, Mappin Street, Sheffield, S1 3JD, UK.

18
19
20

21 Corresponding author: Dr E. Shahabpoor
22 Department of Civil & Structural Engineering
23 University of Sheffield
24 Sir Frederick Mappin Building
25 Sheffield S1 3JD
26 E-mail: e.shahabpoor@sheffield.ac.uk
27 Tel: 0114-2225745
28 Fax: 0114-2225700

29
30
31

32	Body text word count:	7196
33	Number of figures:	11
34	Number of tables:	5

35

36 **Abstract**

37 Predicting the effect of walking traffic on structural vibrations is a great challenge to
38 designers of pedestrian structures, such as footbridges and floors. This is mainly due to the
39 lack of adequate design guidelines, which in turn can be blamed on poor research findings.
40 Even the fundamental data are very rare and limited. This study proposes a new and more
41 reliable method for serviceability assessment of the vertical vibrations induced by multi-
42 pedestrian walking traffic. Key novelties include modelling the natural *variability* of the
43 walking forces and the human bodies, as well as their individual *interaction* with the
44 supporting structure at their *moving location*. Moreover, a novel approach to vibration
45 serviceability assessment (VSA) is proposed based on the actual level of vibration
46 experienced by each pedestrian, rather than the typical maximum vibration response at a
47 fixed point. Application of this method on two full-scale footbridge structures have shown
48 that, with a suitable calibration of human model parameters, the proposed method can
49 predict the occupied structure modal frequency with less than 0.1% error and - more
50 importantly - modal damping ratio with less than 1% error. The new method also estimated
51 the structural responses with considerably less error (5-10%) compared to a selection of
52 current design guidelines (200-500%). The proposed VSA method is not suitable for hand-
53 based calculations. However, if coded and materialised as a user-friendly software, it can
54 be incorporated into design guidelines and used by consultants in everyday engineering
55 practice.

56 **Keywords:** human-induced vibration; walking human model; pedestrian traffic;
57 footbridge;

58 **1 Introduction**

59 Models of pedestrian dynamic loading used in contemporary vibration serviceability
60 assessment typically describe the vertical walking excitation as a vertical force that does
61 not depend on structural vibrations [1]. The simplest models, such as those presented by
62 FIB [2], ISO 10137 [3], French design guideline [4] and UK National Annex to Eurocode
63 1 [5], also assume that an individual walking force is periodic and presentable by a Fourier
64 series. The frequency content of such a simple force model typically contains up to the first
65 four dominant harmonics [1]. The design procedures usually require that one of the
66 harmonics matches the frequency of a target vibration mode of the structure to create
67 resonance, i.e. the worst case scenario yielding the maximum vibration response. To
68 account for the imperfect synchronisation between individuals in a group or crowd, the
69 walking force of a multi-pedestrian traffic is calculated by multiplying a sum of the
70 individual forces with factor(s) which commonly depend only on the number of pedestrians
71 on the structure [1].

72 A significant move towards a more realistic estimation of the vibration response was made
73 only recently, by taking into account inter- and intra- subject variability of the pedestrians
74 in statistical models of their walking force [6-12]. This has increased considerably the
75 fidelity of the walking force models. Yet, these still do not account for human-structure
76 interaction (HSI), despite its widely recognised importance to reliable prediction of the
77 vibration response [13-15]. In the context of the present study, HSI refers to the effect of
78 walking bodies on the dynamic properties of the occupied structure (i.e. modal mass,
79 stiffness and damping).

80 The UK recommendations for the design of permanent grandstands [16] are the only
81 guidelines that explicitly require taking into account the interaction of both passive and
82 active people with the grandstand they occupy and excite by jumping or bouncing in the
83 vertical direction. Based on the model proposed by Dougill, et al. [17], this guideline

84 suggests two single-degree-of-freedom (SDOF) systems attached to a SDOF model of the
85 empty structure to simulate the aggregated effect of passive (mostly *sitting*) and active
86 (mostly *jumping/bouncing*) people. Despite the satisfactory performance of this explicit
87 modelling approach [18, 19], no other vibration serviceability design guideline has yet
88 adopted a similar modelling concept to account for the HSI due to people *walking*.

89 The vibration serviceability assessment (VSA) method proposed in this paper (from now
90 on referred to as *interaction-based VSA method*) has been developed to account for the
91 following five main challenges when assessing the effects of walking people on structures:

- 92 1) The human-structure interaction;
- 93 2) Variability of the mass, stiffness and damping of the moving human body and the
94 walking force due to inter- and intra-subject variability;
- 95 3) Variability of pedestrian traffic characteristics, such as traffic *volume* and *regime*
96 (spatially unconstrained/constrained, group, etc.)
- 97 4) Varying *location* of each walking pedestrian on the structure, and
- 98 5) The actual level of vibration experienced by each pedestrian at their continuously
99 moving location on the structure rather than the vibration response of the structure
100 at a fixed point.

101 The detailed description of the proposed method is presented in Section 2. In Section 3, the
102 sensitivity of the outputs of this method to uncertainties of its inputs is studied. Applications
103 of the proposed *interaction-based VSA method* on two full-scale footbridge structures are
104 described in Section 4, and the relevant response calculations are compared to a selection
105 of current design guidelines. Finally, conclusions are presented in Section 5.

106 **2 Description of assessment method**

107 The proposed interaction-based VSA method involves four steps. In the first step, the
108 effects of HSI are analysed by estimating the *occupied* structure modal properties: natural
109 frequency f_{os} [Hz], modal damping ratio ζ_{os} [-] and modal mass m_{os} [kg]. In the second step,
110 for each relevant mode of the occupied structure, the total modal force due to pedestrian
111 traffic is calculated. This is done by scaling each individual's walking force by the
112 amplitude of the corresponding mode shape, and superimposing such scaled walking forces
113 of all pedestrians according to their arrival time on the structure. In the third step, the modal
114 response of the structure is computed for each relevant mode of vibration, using the
115 calculated modal walking force/s and the *occupied* structure modal properties. Finally,
116 these modal vibration responses are used to calculate the physical vibration levels perceived
117 by each pedestrian at their *continuously changing location* as they walk along the structure.
118 This is deemed to be more appropriate and realistic than using the percentage of time that
119 bridge response is within an acceptable range at a particular fixed location, which may or
120 may not have a pedestrian on it.

121 It should be noted that the description of the interaction-based VSA method in this study is
122 based on a uniformly distributed un-constrained traffic scenario. However, any traffic
123 pattern/scenario can be simulated using this method by modifying the steps to reflect that
124 pattern. For instance, a constrained walking due to heavy traffic can be simulated by
125 reducing the average walking speed of the crowd, increasing the arrival rate and applying
126 corresponding changes on the walking force and parameters of the SDOF walking human
127 model.

128 **2.1 Input parameters**

129 The input parameters used in the interaction-based VSA method can be divided into four
130 categories. The first category comprises the properties of mode 'j' of the *empty* structure:

131 modal mass $m_{es,j}$, frequency $f_{es,j}$ and damping ratio $\zeta_{es,j}$. In the second category are the
132 parameters of the walking human SDOF model: mass m_h , natural frequency f_h and damping
133 ratio ζ_h . The SDOF mass-spring-damper model of walking humans proposed by
134 Shahabpoor, et al. [20] was used in this study (Fig. 1). The authors proposed normal
135 distributions with mean and standard deviations of $\mu=2.85\text{Hz}$ and $\sigma=0.34\text{Hz}$ for natural
136 frequency f_h , and $\mu=0.295$ and $\sigma=0.047$ for damping ratio ζ_h of the SDOF human model.
137 Mass m_h can either be generated using a statistical distribution for a certain human
138 population, or assumed to be equal to the average mass of the occupants. Stiffness k_h can
139 be calculated using Equation (1):

$$140 \quad k_h = m_h(2 \times \pi \times f_h)^2 \quad (\text{Eq. 1})$$

141 The third category of the input parameters is related to the walking traffic. These
142 parameters define the loading scenario in statistical terms. An appropriate traffic pattern
143 first needs to be defined. For instance, it could be a stream of pedestrians with arrival rate
144 r_a [pedestrians/time unit] at the bridge and walking speed v_w [m/s] defined by their
145 corresponding statistical distributions.

146 The last category of inputs is individuals' walking force, which can be either measured or
147 synthetically generated, as described in Section 2.3.

148 **2.2 Step 1: Human-structure Interaction**

149 Important effects of human-structure interaction on modal properties and vibration
150 response of a structure are studied parametrically by the authors elsewhere [21]. The mass
151 of a stationary human body accelerates when exposed to structural vibration, and applies
152 interaction force on the structure [22]. The same applies to the moving body, in which case
153 an additional ground reaction force is created due to the base vibration [23]. Similar to a
154 tuned mass damper, these interaction forces manifest as changes in the modal frequency

155 (i.e. mass and/or stiffness) and damping of the structure. This is because the interaction
156 forces have components proportional to acceleration, velocity and displacement, as well as
157 components independent from the structural movement [1].

158 In reality, pedestrian locations on the structure and, therefore, their interaction with
159 structure, are changing with time. The interaction-based VSA method uses a Monte-Carlo
160 iterative process based on *sampling distribution* concept [24] to estimate the *average* effect
161 of HSI on modal properties of the empty structure.

162 In statistics, a sampling distribution or finite-sample distribution is the probability
163 distribution of a given statistic based on a random sample drawn from a larger data
164 population [24]. According to the statistical inference theory, where the statistic is the
165 sample mean and samples are uncorrelated, the standard deviation of the sampling
166 distribution of a statistic, usually referred to as the standard error of that quantity, is
167 inversely proportional to the square root of the number of samples N [24].

168 The interaction-based VSA method takes into account the HSI effects on the structure by
169 replacing the empty structure modal properties (f_{es} , ζ_{es} and m_{es}) with the corresponding
170 occupied structure modal properties (f_{os} , ζ_{os} and m_{os}). Based on the statistical inference
171 theory, if the occupied structure modal properties f_{os} , ζ_{os} and m_{os} (i.e. samples) are
172 calculated for an increasing number of different walking traffic patterns, the average value
173 of each of f_{os} , ζ_{os} and m_{os} (i.e. statistics), gradually converges to their mean value i.e. the
174 standard error of the statistics decreases.

175 The following steps describe the procedure to estimate the mean values of f_{os} , ζ_{os} and m_{os} :

176 Firstly (Step 1.1), the number of people walking on the structure is selected. This can be
177 based on a statistical distribution of arrival rates and the average crossing time (i.e. the
178 average time needed for a pedestrian to cross the structure). For instance, where the arrival

179 rate is 10 pedestrians per minute and the average crossing time is 2 minutes, under steady
180 state conditions, there would be on average 20 people walking on the structure at any given
181 time, assuming that their walking speeds are equal and constant.

182 Secondly (Step 1.2), a location must be assigned to each person, either randomly (e.g.
183 assuming the uniform distribution), or based on a particular pattern that the loading scenario
184 may require. The location assigned to each person is assumed constant (*stationary*) for that
185 particular moment of time. This is the same as an imaginary case where people are walking
186 on a series of treadmills installed at fixed locations on the structure, in which case their
187 locations on the structure do not change while walking (Fig. 2).

188 The multi-degree of freedom (MDOF) model of a ‘stationary’ multi-pedestrian walking
189 traffic-structure system is developed in Step 1.3. An SDOF model is used to simulate each
190 walking individual on the structure (Fig. 1). Similarly, an SDOF model is used to simulate
191 one mode of the empty structure at a time. The effects of the constant location of each
192 person on the modal properties of the occupied structure are taken into account by using
193 the structure mode shape ordinate at the location of each person [20].

194 By coupling a number of SDOF systems representing walking individuals and an SDOF
195 system representing a mode of the structure, the proposed modelling approach essentially
196 bridges the modal domain and the physical domain. Therefore, the modal properties of the
197 structure and its mode shape have to have ‘physically’ meaningful values. To ensure that
198 modal properties of the crowd-structure system are found with the same scaling as for the
199 empty structure the *unity-normalised* mode shapes at the structural DOF must consistently
200 be used throughout the calculations.

201 Being stationary in the current time-step, the walking traffic-structure system shown in Fig.
202 1 can be treated as a conventional multiple degree of freedom (MDOF) system [25].

$$203 \quad [M]\{\ddot{x}(t)\} + [C]\{\dot{x}(t)\} + [K]\{x(t)\} = \{F(t)\} \quad (\text{Eq. 2})$$

204 The following modified system of equations of motion (Eq. 3) can be used to account for
 205 the locations of the pedestrians:

$$\begin{aligned}
 206 \quad & \begin{bmatrix} m_{es,j} & 0 & 0 & \cdots & 0 \\ 0 & m_{h1} & 0 & \cdots & 0 \\ 0 & 0 & m_{h2} & \cdots & 0 \\ \vdots & \vdots & \vdots & \ddots & \vdots \\ 0 & 0 & 0 & \cdots & m_{hn} \end{bmatrix} \begin{bmatrix} \ddot{x}_{os,j}(t) \\ \dot{x}_{h1}(t) \\ \dot{x}_{h2}(t) \\ \vdots \\ \dot{x}_{hn}(t) \end{bmatrix} + \\
 207 \quad & \begin{bmatrix} c_{es,j} + (c_{h1} \times \phi_{1j}) + (c_{h2} \times \phi_{2j}) + \cdots + (c_{hn} \times \phi_{nj}) & -(c_{h1} \times \phi_{1j}) & -(c_{h2} \times \phi_{2j}) & \cdots & -(c_{hn} \times \phi_{nj}) \\ & -(c_{h1} \times \phi_{1j}) & c_{h1} & 0 & \cdots & 0 \\ & -(c_{h2} \times \phi_{2j}) & 0 & c_{h2} & \cdots & 0 \\ & \vdots & \vdots & \vdots & \ddots & \vdots \\ & -(c_{hn} \times \phi_{nj}) & 0 & 0 & \cdots & c_{hn} \end{bmatrix} \begin{bmatrix} \dot{x}_{os,j}(t) \\ \dot{x}_{h1}(t) \\ \dot{x}_{h2}(t) \\ \vdots \\ \dot{x}_{hn}(t) \end{bmatrix} + \\
 208 \quad & \begin{bmatrix} k_{es,j} + (k_{h1} \times \phi_{1j}) + (k_{h2} \times \phi_{2j}) + \cdots + (k_{hn} \times \phi_{nj}) & -(k_{h1} \times \phi_{1j}) & -(k_{h2} \times \phi_{2j}) & \cdots & -(k_{hn} \times \phi_{nj}) \\ & -(k_{h1} \times \phi_{1j}) & k_{h1} & 0 & \cdots & 0 \\ & -(k_{h2} \times \phi_{2j}) & 0 & k_{h2} & \cdots & 0 \\ & \vdots & \vdots & \vdots & \ddots & \vdots \\ & -(k_{hn} \times \phi_{nj}) & 0 & 0 & \cdots & k_{hn} \end{bmatrix} \begin{bmatrix} x_{os,j}(t) \\ x_{h1}(t) \\ x_{h2}(t) \\ \vdots \\ x_{hn}(t) \end{bmatrix} = \\
 209 \quad & \begin{bmatrix} F_{ex,j}(t) + (F_{h1}(t) \times \phi_{1j}) + (F_{h2}(t) \times \phi_{2j}) + \cdots + (F_{hn}(t) \times \phi_{nj}) \\ 0 \\ 0 \\ \vdots \\ 0 \end{bmatrix} \quad (\text{Eq. 3})
 \end{aligned}$$

210 where $m_{es,j}$, $c_{es,j}$ and $k_{es,j}$ are the modal mass, damping and stiffness for the j^{th} mode of
 211 the empty structure and m_{hi} , c_{hi} and k_{hi} are those of the walking individuals. Viscous
 212 damping is assumed for SDOF walking human models. $\ddot{x}_{os,j}(t)$, $\dot{x}_{os,j}(t)$ and $x_{os,j}(t)$ are,
 213 respectively, the acceleration, velocity and displacement response of the occupied structure
 214 DOF. As one mode of the occupied structure (j) is simulated at a time, $\ddot{x}_{os,j}(t)$, $\dot{x}_{os,j}(t)$
 215 and $x_{os,j}(t)$ represent the *modal* response of the occupied structure. Similarly, $\ddot{x}_{hi}(t)$,
 216 $\dot{x}_{hi}(t)$ and $x_{hi}(t)$ represent the acceleration, velocity and displacement of the i^{th} walking
 217 person DOF. $F_{ex,j}(t)$ is the mode ' j ' modal force (if any), due to an external force acting
 218 on the structural DOF, and $F_{hi}(t)$ is a walking force of person ' i ' on a stiff surface.
 219 Meanwhile, ϕ_{ij} is the ordinate of the ' j^{th} ' mode shape of the structure at the location of
 220 person ' i ' in the current time-step.

221 The damping matrix in Equation (3) is normally not proportional. Therefore, the
 222 conventional formulation of the proportionally-damped eigenvalue problem [25] will not
 223 yield modal vectors (eigenvectors) that uncouple the equations of motion of the system.
 224 The state-space technique used here to overcome this problem was first documented by
 225 Frazer, et al. [26] and involves the reformulation of the original equations of motion, for an
 226 N-degree of freedom system, into an equivalent set of 2N first order differential equations.
 227 In the first step, a new coordinate vector $\{y(t)\}$ containing displacement $\{x(t)\}$ and
 228 velocity $\{\dot{x}(t)\}$ is defined:

$$229 \quad \{y(t)\} = \begin{Bmatrix} x(t) \\ \dot{x}(t) \end{Bmatrix} \quad (\text{Eq. 4})$$

230 Then Equation (2) is re-written into the following form for modal analysis:

$$231 \quad \begin{bmatrix} [C] & [M] \\ [M] & [0] \end{bmatrix} \{y(t)\} + \begin{bmatrix} [K] & [0] \\ [0] & [-M] \end{bmatrix} \{y(t)\} = \{0\} \quad (\text{Eq. 5})$$

232 Where [M], [C] and [K] matrices are the mass, damping and stiffness matrices of the traffic-
 233 structure system, accordingly, as defined in Equation (3).

234 By defining α and β matrices as:

$$235 \quad \alpha = \begin{bmatrix} [C] & [M] \\ [M] & [0] \end{bmatrix}, \quad (\text{Eq. 6})$$

$$236 \quad \beta = \begin{bmatrix} [K] & [0] \\ [0] & [-M] \end{bmatrix} \quad (\text{Eq. 7})$$

237 Equation (5) leads to a standard eigenvalue problem in the form of Equation (8).

238 $(\mathbf{s}\boldsymbol{\alpha}+\boldsymbol{\beta})\boldsymbol{\psi}=0$ (Eq. 8)

239 The complex valued eigenvectors $\boldsymbol{\psi}$ (mode shapes) and real valued eigenvalues \mathbf{s} (modal
240 frequencies) in Equation (8) can be found by solving the corresponding characteristic
241 polynomial equation:

242 $\det(\mathbf{s}\boldsymbol{\alpha}+\boldsymbol{\beta})=0$ (Eq. 9)

243 This yields natural frequencies, modal damping ratios and modal masses of the non-
244 proportionally damped pedestrian traffic-structure MDOF system. Further discussion of
245 modal analysis of systems with non-proportional damping is beyond the scope of this paper.

246 The MDOF system in Fig. 1 has $n+1$ modes of vibration. The *dominant mode* of vibration
247 is defined as the mode with the maximum response at the ‘structure’ degree of freedom.

248 By repeating the process of eigenvalue extraction (Steps 1.1 – 1.3) for different
249 combinations of pedestrian traffic parameters (number of pedestrians on the structure, their
250 location, etc.) and calculating the average values of f_{os} , ζ_{os} and m_{os} corresponding to
251 increasing number of iterations, they each gradually converge to constant values. Fig. 3
252 illustrates the convergence of f_{os} and ζ_{os} for a typical simulation involving 800 different
253 locations of pedestrians. These converged modal properties of the occupied structure are
254 then used in the response calculation instead of those of the empty structure. The
255 calculation is not computationally demanding and can be completed within several seconds
256 using a standard PC configuration.

257 **2.3 Step 2: Generating modal force of multi-pedestrian walking traffic**

258 The second step is to generate the modal force due to multi-pedestrian walking traffic. Most
259 of the parameters of the walking traffic, such as arrival rate r_a , arrival time t_a , location,
260 walking speed $v_w(t)$ and

261 walking force $F_w(t)$ of individuals, are time-varying and inherently stochastic. This makes
262 it impossible to predict the exact traffic force at any particular time. The way forward is to
263 treat it statistically. The step-by-step procedure for generating modal force due to walking
264 traffic is elaborated in the following paragraphs.

265 First (Step 2.1), the duration of the simulated vibration response is selected randomly. A
266 criterion is introduced in Step 4 (Section 2.5) to check whether the selected duration is
267 sufficiently long. In physical terms, this criterion ensures that the structure experiences
268 enough variations of the walking traffic loading necessary to assess the vibration
269 serviceability of the structure. In case the duration in Step 2.1 proves to be insufficient in
270 Step 4, it must be increased and Steps 2-4 repeated.

271 In Step 2.2, the number of people entering the structure needs to be selected, using a
272 statistical distribution of their arrival rate. Then, the arrival time is assigned randomly to
273 each pedestrian. For instance, assuming uniform distribution for an arrival rate of 4
274 pedestrians per minute, entering the structure between minute 12 and 13 of the simulation,
275 their random arrival times could be 12:03, 12:12, 12:38 and 12:51.

276 In Step 2.3, a constant walking speed (v_w) needs to be selected for each pedestrian, using a
277 statistical distribution, such as the one reported by Zivanovic [27]. It is assumed that v_w is
278 constant for each pedestrian, but it varies between pedestrians. Having the walking speed
279 and the length of structure i.e. walking path, the duration of walking of each pedestrian (so
280 called 'crossing time') can be computed. For instance, if the pedestrian speed is $v_w=1.8$ m/s
281 and the structure length is 36 meters, it takes 20s for that person to cross.

282 A walking force needs to be assigned to each pedestrian in Step 2.4. The duration of the
283 walking force for each person should be equal to the crossing time of that person. As
284 previously mentioned, either an experimentally recorded [28] or a synthetically generated
285 walking force can be used in the simulation. If a walking force is to be generated artificially,

286 it is important to use a method that takes into account the inter- and intra-subject variability
 287 of the walking force and realistically simulates its frequency contents, such as those
 288 proposed by Zivanovic, et al. [7] and Racic and Brownjohn [6].

289 As pedestrians walk along the structure, their location and the level of interaction with it
 290 change. To account for this, the walking force of each individual 'i' $F_{w,hi}(t)$, entering the
 291 structure at $t = t_{ai}$ and leaving it at $t = t_{bi}$ is scaled with $\phi_{ij}(t)$ which is the amplitude of
 292 the unity-scaled shape of mode 'j' of the structure at the instantaneous location of the
 293 moving pedestrian 'i' at time 't'. This yields the modal walking force of human 'i' exciting
 294 mode 'j' of the structure $F_{w,hi \rightarrow sj}(t)$:

$$295 \quad F_{w,hi \rightarrow sj}(t) = \begin{cases} 0 & t < t_{ai} \\ \phi_{ij}(t) \times F_{w,hi}(t) & t_{ai} \leq t \leq t_{bi} \\ 0 & t_{bi} < t \end{cases}, \quad (\text{Eq. 10})$$

296 Where $\phi_{ij}(t)$ is defined as:

$$297 \quad \phi_{ij}(t) = \begin{cases} 0 & t < t_{ai} \\ \sin\left(\frac{t-t_{ai}}{t_{bi}-t_{ai}}j\pi\right) & t_{ai} \leq t \leq t_{bi} \\ 0 & t_{bi} < t \end{cases}, \quad (\text{Eq. 11})$$

298 assuming that the structure mode shape is sinusoidal and the walking speed is constant. For
 299 other mode shapes, such as those calculated via FE analysis, a mode shape vector can be
 300 used in Equation (11).

301 Fig. 4a presents a typical walking force of an individual, scaled by the amplitude of the first
 302 unity-normalised mode shape of a simply supported beam structure. This person crosses
 303 the structure in 10.4s. It is assumed that the empty structure mode shape does not change
 304 when occupied by walking people [20].

305 Finally, in Step 2.6, the modal walking forces of all ' n ' pedestrians are superimposed, based
306 on their arrival time on the structure, to generate the modal force of the walking traffic
307 experienced by the mode ' j ' of the structure $F_{w,t \rightarrow sj}(t)$:

$$308 \quad F_{w,t \rightarrow sj}(t) = F_{w,h1 \rightarrow sj}(t) + F_{w,h2 \rightarrow sj}(t) + \dots + F_{w,hn \rightarrow sj}(t) \quad (\text{Eq. 12})$$

309 Fig. 4 presents a typical superposition process, where modal forces due to walking of three
310 individual pedestrians (Fig. 4a, b and c) are superimposed to generate the modal force of
311 the walking traffic (Fig. 4d). Pedestrians 1, 2 and 3 arrive on the structure at $t_a = 2, 6$ and 8 s
312 respectively and each take 10.4 s to cross the structure. Steps 2.5 and 2.6 need to be repeated
313 for all relevant modes of structural vibration.

314 **2.4 Step 3: Calculating structural modal response**

315 Here, the modal force of the walking traffic $F_{w,t \rightarrow sj}(t)$, calculated in Step 2 (Section 2.3),
316 is applied on the corresponding mode ' j ' of vibration ($m_{os,j}$, $\omega_{os,j}$ and $\zeta_{os,j}$) of the occupied
317 structure, calculated in Step 1 (Section 2.2), to calculate the modal response. This can be
318 done using a conventional closed form method such as convolution or numerical integration
319 such as Newmark-beta and Runge-Kutta methods [25]. Step 3 is repeated for all modes and
320 the resulting modal responses are calculated.

321 **2.5 Step 4: Serviceability assessment**

322 The Cumulative Distribution Function (CDF) of an acceleration response at a particular
323 pre-defined fixed location on the structure - referred to as *fixed-location (FL) CDF* in this
324 paper - is commonly used to assess vibration serviceability [7,8]. It provides a probability
325 of non-exceedance for any particular response amplitude at a specific fixed location on the
326 structure [29]. However, FL CDF is misleading in scenarios where traffic volume is not
327 constant on the structure. Moreover, it does not take into account the location of pedestrians

328 on the structure and the changing level of vibration they actually experience while in
329 motion.

330 To address these issues, the novel concept of *moving-location (ML) CDF* is introduced here
331 and used in the interaction-based VSA method. ML CDF addresses the disadvantages of
332 the FL CDF by taking into account the number and moving location of pedestrians on the
333 structure at each moment of time. ML CDF further takes into account the level of
334 acceleration response experienced by each pedestrian while moving over the structure
335 rather than structural response at a fixed location, which may or may not be experienced
336 by pedestrians.

337 To calculate the ML CDF, in the first step, the time-history of the vibration levels
338 experienced by each pedestrian needs to be simulated. Fig. 5 shows the process of
339 calculating the time-history of the acceleration response of structure $\ddot{x}_{s \rightarrow hi}(t)$ experienced
340 by a typical pedestrian ‘*i*’ crossing a beam-like simply supported structure. Only the first
341 two vertical modes of structural vibration were considered relevant for this example. Each
342 pedestrian’s experience of vibration response created by each mode (blue traces in Fig. 5a
343 and Fig. 5b) can be calculated by scaling the modal response $\ddot{x}_{os,j}(t)$ (grey traces in Fig.
344 5a and Fig. 5b) of the structure (pertinent to the time window during which the pedestrian
345 is walking on the structure) by its corresponding $\phi_{ij}(t)$ (red traces in Fig. 5a and Fig. 5b).
346 The total acceleration response of the structure experienced by moving pedestrian ‘*i*’
347 $\ddot{x}_{s \rightarrow hi}(t)$ can be calculated by adding up his/her experience of vibration response due to all
348 relevant modes, as shown in Equation (13):

$$349 \quad \ddot{x}_{s \rightarrow hi}(t) = \begin{cases} 0 & t < t_{ai} \\ \sum_j [\phi_{ij}(t) \times \ddot{x}_{os,j}(t)] & t_{ai} \leq t \leq t_{bi} \\ 0 & t_{bi} < t \end{cases} \quad (\text{Eq. 13})$$

350 For example, the pedestrian shown in Fig. 5 enters the structure at $t_a=6s$, and they need
 351 10.4s to cross the beam structure. Fig. 5a and Fig. 5b show the time histories of the physical
 352 vibration (blue traces in Fig. 5) that the pedestrian experiences due to mode 1 and 2,
 353 respectively. The response of each mode ‘j’ $\ddot{x}_{os,j}(t)$ (grey curve) is multiplied by the
 354 corresponding $\phi_{ij}(t)$ (red curve), starting at $t_a=6s$, with a duration of 10.4s to make this
 355 calculation. The two time histories are then superimposed in time to generate the time
 356 history of the total physical vibration experienced by the pedestrian (Fig. 5c).

357 If this process is repeated for all pedestrians crossing the structure and the time histories of
 358 their experiences are connected together in series, as shown in Fig. 5d, the time history
 359 containing levels of vibration that the pedestrian traffic experienced during their crossing
 360 $\ddot{x}_{s \rightarrow t}(t)$ is created. Such a method of calculating $\ddot{x}_{s \rightarrow t}(t)$ not only takes into account the
 361 actual level of vibration each pedestrian experiences based on their moving location on the
 362 structure, but also takes into account the duration in which each pedestrian is exposed to a
 363 certain level of vibration.

364 *ML CDF* is defined as the CDF of all samples in $\ddot{x}_{s \rightarrow t}(t)$ time history. For any particular
 365 amplitude of $\ddot{x}_{s \rightarrow t}(t)$, ML CDF ordinate provides the probability that a pedestrian does not
 366 experience a vibration level higher than the selected amplitude.

367 Using a typical example and assuming a single mode response, Fig. 6 compares the
 368 performance of the FL (at anti-node) and ML CDFs in the assessment of vibration
 369 serviceability. The acceleration response of the structure is given for 60 minutes for two
 370 loading scenarios A and B. As can be seen in Fig. 6a and Fig. 6c, the mean arrival rate in
 371 scenario A is constant (20 pedestrians / minute) whereas in scenario B it shows a 6 fold

372 increase from 10 peds/min to 70 peds/min in the last 10 minutes. A considerable difference
373 between FL and ML CDFs is noticeable in both scenarios (Fig. 6b and Fig. 6d). In Scenario
374 A, neglecting the location of people on the structure results in an over-estimation of the
375 response in the FL CDF (Fig. 6b - blue trace). In Scenario B, the change of traffic volume
376 amplifies the over-estimation problem (Fig. 6d - blue trace). For example, based on Fig.
377 6d, if 0.2 m/s^2 is selected arbitrarily as the maximum acceptable response, the maximum
378 structural response at the fixed location would be acceptable for only 60% of the time (FL
379 CDF) with, or more likely, without having any pedestrians experiencing that vibration.
380 However, according to ML CDF the 0.2 m/s^2 response is acceptable for 80% of the total
381 time, during which pedestrians experience vibrations while crossing the footbridge. There
382 is a considerable difference between FL and ML CDF interpretations

383 As discussed in Section 2.3, since the pedestrian traffic on the structure is being treated
384 statistically (walking speed, location, arrival time, etc.), the duration of the response
385 simulation needs to be sufficiently long to ensure that the structure has experienced enough
386 variations of the walking traffic loading necessary to assess its vibration serviceability. To
387 check this sufficiency, the *sampling distribution* concept [24] is used again.

388 In statistical terms, the calculated time-history of traffic vibration experience $\ddot{x}_{s \rightarrow t}(t)$ and
389 its corresponding ML CDF parameters is a finite sample from a larger population of
390 possible vibration responses experienced by pedestrians. Assuming the statistic as the *mean*
391 response amplitudes corresponding to 95%, 85%, 75% and 50% probability of non-
392 exceedance ($a_{95\%}$, $a_{85\%}$, $a_{75\%}$ and $a_{50\%}$) corresponding to the CDF, the standard deviation
393 (error) of these mean response amplitudes is inversely proportional to square root of data
394 samples N (which is proportional to the duration of the response simulation) as N increases.
395 In other words, the longer the duration of the response simulation, the $\ddot{x}_{s \rightarrow t}(t)$ contains the
396 vibration experience of more pedestrians and therefore can represent more accurately and
397 reliably the vibration response of the structure in probabilistic terms.

398 For the interaction-based VSA method suggested in this study, it is proposed to select the
399 duration of the response simulation (Section 2.3) in a way to get the standard errors ' $\bar{\sigma}$ ' less
400 than 5% of the corresponding $a_{95\%}$, $a_{85\%}$, $a_{75\%}$ and $a_{50\%}$ mean values. The standard errors $\bar{\sigma}$
401 of the $a_{95\%}$, $a_{85\%}$, $a_{75\%}$ and $a_{50\%}$ values of the response ML CDF can be checked by
402 monitoring their variations for increasing the length of the time window of the response
403 being analysed. Fig. 7 presents a typical fluctuation of the mean $a_{95\%}$, $a_{85\%}$, $a_{75\%}$ and $a_{50\%}$ for
404 up to 14 hours of the simulated response. The length of the time window of vibration
405 response (t_w) (and therefore number of samples N) used for calculating $a_{95\%}$, $a_{75\%}$, $a_{75\%}$ and
406 $a_{50\%}$ was increased in each iteration by 75s, yielding: $t_{w1}=75s$, $t_{w2}=150s$, $t_{w3}=225s$, etc. In
407 the case of the response illustrated in Fig. 7, $\bar{\sigma}$ of the mean $a_{95\%}$, $a_{85\%}$, $a_{75\%}$ and $a_{50\%}$ reduced
408 to below 5% of their mean value after fewer than 500 iterations. This is equivalent to 10h
409 and 25mins of the simulated response, which a standard office PC can process in just a
410 couple of minutes. . If $\bar{\sigma}$ values do not reduce to less than 5% of their mean value at the end
411 of the simulation, the simulation duration determined in the Step 2 needs to be increased
412 and Steps 2-4 repeated until $\bar{\sigma}$ meet the 5% error criteria.

413 **3 Sensitivity analysis**

414 As this is a new and untested methodology, this section examines the sensitivity of the
415 outputs of the proposed method to its inputs. The human model parameters (f_h , ζ_h and m_h),
416 mean arrival rate r_a and walking speed v_w were selected as input parameters. The selected
417 outputs were the occupied structure modal parameters f_{os} and ζ_{os} , response amplitude with
418 a 95% chance of non-exceedance $a_{95\%}$ and RMS of the total response time-history a_{rms} . The
419 selected input parameters were varied by $\pm 25\%$ or $\pm 30\%$ and their effects on the outputs
420 were analysed. In order to compare the sensitivity of each output parameter with different
421 inputs, all parameters were normalised by the corresponding baseline (minimal) value. The
422 baseline values were adopted from a real-world structure and a realistic traffic scenario as

423 follows: $f_{h,base}=2.85\text{Hz}$, $\zeta_{h,base} =0.295$, $m_{h,base} =75\text{kg}$, $r_{a,base}=0.35\text{ped/s}$, $v_{w,base}=1.38\text{m/s}$,
424 $f_{os,base}=2.03\text{Hz}$, $\zeta_{os,base}=0.007$, $a_{95\%,base}=0.341\text{m/s}^2$ and $a_{rms,base}=0.155\text{m/s}^2$.

425 Fig. 8 presents sensitivity curves for each normalised output parameter: $f_{os}/f_{os,base}$, $\zeta_{os}/\zeta_{os,base}$,
426 $a_{95\%}/a_{95\%,base}$ and $a_{rms}/a_{rms,base}$. The horizontal axis shows the normalised input parameters
427 $f_h/f_{h,base}$, $\zeta_h/\zeta_{h,base}$, $m_h/m_{h,base}$, $r_a/r_{a,base}$, and $v_w/v_{w,base}$. As can be seen in Fig. 8a, the natural
428 frequency of the occupied structure, f_{os} , shows low sensitivity to the variation of all input
429 parameters. On the other hand, Fig. 8b shows that the occupied structure damping ratio ζ_{os}
430 is highly sensitive to the human model natural frequency f_h when f_h is very close to the
431 modal frequency of the empty structure f_{es} . For instance, when $f_h/f_{h,base} = 0.8$ ($f_h=2.28$ Hz
432 and relatively close to $f_{es} =2.04$ Hz), ζ_{os} increases by 65% compared to its base value $\zeta_{os,base}$
433 (i.e. $\zeta_{os}/\zeta_{os,base} =1.65$). When f_h and f_{es} are not very close, ζ_{os} is not very sensitive to f_h . This
434 also yields the high sensitivity of $a_{95\%}$ and a_{rms} to f_h (blue curve in Fig. 8c and d) when f_h
435 and f_{es} are very close. Apart from the effects of f_h , a 30% variation in the rest of the input
436 parameters (m_h , ζ_h , r_a and v_w) changed the response up to only 10%. In this sense, the
437 method shows a high level of robustness to uncertain inputs.

438 **4 Experimental verification**

439 To examine the performance of the interaction-based VSA method, a set of tests was
440 carried out on two full-scale footbridges: a post-tensioned concrete footbridge at the
441 University of Sheffield (Fig. 9a) and a steel box girder footbridge located in Podgorica,
442 capital of Montenegro (Fig. 9b) [30]. The modal frequency, damping ratio and modal mass
443 of the first vertical mode of the Sheffield footbridge are: 4.44Hz, 0.6% and 7,128kg,
444 respectively [20]. For the Podgorica footbridge these parameters are: 2.04Hz, 0.26% and
445 58,000kg, respectively [30]. Both structures are very lightly damped, and have natural
446 frequencies in the range excitable by walking forces. Moreover, their natural frequencies
447 are close to the natural frequency of the walking human SDOF model. This yields a high

448 level of interaction between pedestrians and structure, based on the analogies presented by
449 Shahabpoor, et al. [21]. In this study, only the first vertical bending mode of vibration was
450 considered for both footbridges.

451 **4.1 Vibration monitoring**

452 Three tests were carried out on the Sheffield footbridge with three (Test 1), six (Test 2) and
453 10 (Test 3) pedestrians walking in a closed-loop path along the full length of the footbridge
454 [20]. The participants were asked to walk at their normal speed and they were free to pass
455 each other. Each test was run for at least 120s. The body mass of each pedestrian was
456 measured using a medical scale. Moreover, in a separate set of tests their walking forces on
457 a stiff surface were recorded using an instrumented treadmill [6]. A pair of PeCo laser
458 pedestrian counters [31], installed at both edges of the footbridge over the walkway, was
459 used to record in real-time the location, walking direction and walking speed of each
460 individual on the structure. Statistical parameters of pedestrian traffic corresponding to
461 Tests 1-3 are presented in Table 1. A normal distribution was found suitable to describe the
462 walking speed of pedestrians. For the average walking speed of 1.28 m/s, an average
463 pedestrian needed 8.4 s to cross the 10.8m support-to-support length of the footbridge.
464 Detailed descriptions of the tests and statistical analyses of traffic parameters are presented
465 elsewhere [32].

466 Similar to the Sheffield tests, three monitoring tests, referred to as Tests 4, 5 and 6 and each
467 lasting 44 minutes, were carried out on the Podgorica footbridge under normal pedestrian
468 traffic. The flow of traffic was recorded using two video cameras located at both ends of
469 the footbridge and synchronised with the recorded acceleration response. Pedestrians'
470 crossing time, average speed and pacing frequency and the number of people on the
471 structure at any particular moment were found using time-stamped video footage [27]. The
472 statistical parameters of the pedestrian traffics for these three tests are adopted from

473 Zivanovic [27] and are presented in Table 1. A normal distribution was found suitable to
474 describe the walking speed and number of people on the footbridge, while a Poisson
475 distribution was used to describe the arrival rate. The average speed of the pedestrians was
476 found to be 1.39 m/s. This means that, on average, a person needs about 75s to cross this
477 104m long bridge. Detailed descriptions of the tests and statistical analyses of traffic
478 parameters are presented elsewhere [27].

479 In both the Sheffield and Podgorica tests, the acceleration response of the structure was
480 recorded at mid-span (the anti-node of the mode 1). The statistical parameters of the
481 structural response for all tests are presented in Table 2.

482 **4.2 Vibration serviceability assessment**

483 The interaction-based VSA method was used to assess the vibration serviceability of both
484 structures for all six tests. The results were compared with the counterparts obtained from
485 widely used design guidelines. Table 3 presents the input parameters used in the
486 interaction-based VSA method to simulate traffic in Tests 1-6. For the Sheffield tests (Tests
487 1-3), the walking forces of the test subjects recorded separately with the instrumented
488 treadmill were used in the simulations. However, in the Podgorica tests (Tests 4-6) such
489 data were not available. Hence, the walking forces were randomly selected from the
490 database of 1,200 force records [6] so that the average static component (i.e. body weight)
491 of the recorded walking forces was equal to the average weight of the pedestrians in each
492 test. The mass m_h , natural frequency f_h and damping ratio ζ_h of the SDOF walking human
493 model, were adapted from Shahabpoor, et al. [20].

494 To estimate the modal parameters of the occupied structures (Step 1), 800 iterations were
495 carried out for each of the six tests, with a varying number of people and their locations on
496 the structure. Such calculated modal parameters for both occupied structures are presented
497 in Table 4 for all six tests.

498 For each of the Tests 1-3 on the Sheffield footbridge, an identical setup (same people,
499 equipment setup, walking path, walking speed, etc.) was used in a forced FRF measurement
500 test. In these tests, the structure was excited in resonance using an electrodynamic shaker,
501 connected to the structure at the anti-node of the target mode while test subjects were
502 walking on the structure. The resulting FRFs from each of these tests were curve-fitted to
503 find the occupied structure (experimental) modal properties. These values are reported in
504 Table 4. The detailed description of these FRF tests and the identification procedure of
505 occupied structure modal properties are presented in [32].

506 As can be seen in Table 4, the interaction-based VSA method has estimated the occupied
507 modal properties of the Sheffield footbridge with very high accuracy. The factors leading
508 to such a good performance of the method are as follows. Firstly, the Sheffield footbridge
509 is a clean beam-like structure with very straightforward dynamics and accurately measured
510 modal properties. Secondly, the tests were carried out under controlled laboratory
511 conditions, resulting in very accurate walking traffic parameters used for HSI simulation.
512 Finally, the human model parameters proposed in [20] and used in this study for human-
513 structure simulations are the results of extensive studies carried out on this particular
514 footbridge. Although the data pertinent to the Tests 1-3 are not used as part of these studies,
515 it is expected that the method will work better than average on this footbridge. However,
516 as can be seen in Table 4, the interaction-based method also performs well in estimating
517 the damping ratio of the occupied Podgorica footbridge where none of the above listed
518 conditions apply.

519 In total, 15 hours of structural response was simulated in Step 3 (see Section 2.4) for each
520 test to ensure the standard error $\bar{\sigma}$ values of the mean $a_{95\%}$, $a_{85\%}$, $a_{75\%}$ and $a_{50\%}$ are below 5%
521 of their mean values. The duration of the available experimentally *measured* responses (2
522 minutes for Tests 1-3 and 44 minutes for Tests 4-6), however, were found insufficient to
523 get the standard errors below 5%, as discussed in Section 2.5. Therefore, the CDF of the

524 measured responses could not be directly compared with the CDF of the simulated
525 response.

526 For such scenarios, it is proposed that a conclusion of *statistical inference* theory called
527 *interval estimation* be used. Interval estimation uses sample data to calculate an *interval* of
528 possible (or probable) values of an unknown *population* parameter so that, under repeated
529 sampling of such datasets, such intervals would contain the true parameter value with the
530 probability at the stated *confidence level* [33, 34].

531 For the purpose of the proposed Interaction-based VSA method, the population is defined
532 as the full length of the simulated response with $\bar{\sigma} < 0.05\mu$ and the sample is a random block
533 (window) of data from this response. The length of each sample block is taken to be equal
534 to the corresponding *measured* response. For instance, for each of the Tests 1-3, the
535 corresponding 15 hours of the simulated response is the population and any randomly
536 selected 2-minute block from these 15h responses is sample data. Similarly, for Tests 4-6,
537 any randomly selected 44-minute block of the corresponding 15h of the simulated
538 responses is sample data.

539 For each test, all possible sample data (2 minutes duration for Tests 1-3 and 44 minutes
540 duration for Tests 4-6) with a maximum 95% overlap were drawn from the corresponding
541 15h simulated structural response (population). The CDF of each of these sample data were
542 calculated. For each response value on the horizontal axis of the CDF, the confidence
543 interval $[\mu - 2\sigma, \mu + 2\sigma]$ is calculated using the corresponding values on all samples' CDFs.
544 The lower and upper limits of the confidence intervals form two new CDF curves (Fig. 10
545 - two dashed red curves) representing the corresponding lower and upper confidence limits
546 of the original CDF curves. Conceptually, this means that for any arbitrary 2-minutes
547 response measurement on the Sheffield footbridge and 44-minute measurements on the
548 Podgorica footbridge, the structural response CDF will be between the lower and upper

549 confidence limit CDFs (Fig. 10 - two dashed red curves) with approximately 95%
550 probability (assuming normal distribution of data points).

551 The results of these simulations are presented in Table 5 and Fig. 10 for Tests 1-6. As can
552 be seen in Fig. 10, the experimental CDF in all tests (blue curve) is within the predicted
553 confidence interval for the CDFs (two dashed red curves). In addition, it can be seen that
554 the experimental CDFs are closer but still above the lower confidence limit CDF. This
555 means that for any arbitrary response level, the probability of non-exceedance estimated by
556 the proposed model will be slightly lower than the actual value, resulting in a reasonably
557 conservative design.

558 To assess the significance of the HSI, identical simulations were repeated for each test
559 without taking into account the interaction effects. Here, empty structure modal properties
560 were used in simulations instead of the occupied structure modal properties. Everything
561 else was assumed to be the same. Fig. 10 demonstrates a significantly better performance
562 of the interaction-based VSA method (solid red curve) compared with its non-interactive
563 counterpart (green curve). It clearly shows the importance of the HSI in predicting response
564 levels and explains the frequent overestimation of responses due to the multi-pedestrian
565 excitation of footbridges when HSI is not taken into account.

566 **4.3 Comparison with design guidelines**

567 The performance of the interaction-based VSA method was further compared with a
568 number of the relevant design guidelines: ISO 10137 standard [3], French road authorities
569 standard [4], UK National Annex to Eurocode 1 [5] and a method proposed by Butz [35].
570 For each test, the input parameters of the design guidelines were selected in a way to
571 simulate as best as possible (within the provision of the guidelines) the corresponding
572 walking traffic. The extensive discussion of the selected guidelines and their shortcomings

573 were presented by Shahabpoor and Pavic [15] and Zivanovic, et al. [14] and are not
574 repeated here.

575 Setra and Butz methods use response amplitude, with 95% probability of non-exceedance
576 ($a_{95\%}$) for assessment. ISO uses peak response and UK NA suggests a mean response plus
577 2.5 times standard deviation ($a_{2.5\sigma}$) for a serviceability assessment. The results of the
578 interaction-based VSA method were calculated based on the FL CDF corresponding to the
579 anti-node response to be able to compare them with the results of the selected guidelines.
580 The interaction-based VSA method results were also compared with their non-interactive
581 counterparts for all tests. As can be seen in Fig. 11, the accuracy of the interaction-based
582 VSA method in predicting structural response is considerably higher than all other methods
583 in all six tests. Comparing like with like, Setra, ISO, UK NA and Butz methods have a 300-
584 700%, 200-500%, 100-400% and 50-100% error in estimating structural response,
585 respectively. This error range is 100-200% for the non-interactive method. In comparison,
586 the interaction-based VSA method results show a maximum 10% error in estimating $a_{95\%}$,
587 $a_{2.5\sigma}$ and a_{rms} and a maximum 30% error in estimating peak acceleration a_{peak} .

588 **5 Conclusions**

589 The interaction-based VSA method proposed in this paper addresses the most important
590 shortcoming of the current vibration serviceability assessment guidelines for pedestrian
591 structures: neglecting the HSI and inter- and intra-subject variability of the walking load
592 and human body parameters. Similar to the successful modelling approach featured in the
593 UK recommendation for the design of permanent grandstands [16], an SDOF mass-spring-
594 damper model and the associated walking forces are used to describe each walking
595 pedestrian on the structure. The key novelties of the method are:

596 1) It takes into account the individual interaction of pedestrians with the structure;

- 597 2) It takes into account the moving location of each pedestrian on the structure,
598 making it possible to assess the actual level of vibration response experienced by
599 each pedestrian while walking on the structure; and
- 600 3) It features a novel vibration assessment method based on this individualised
601 experience of pedestrians from structural vibration. This is a considerable
602 improvement compared with the conventional VSA methods that calculate
603 structural vibration at a particular fixed point, which may or may not be
604 experienced by the users.

605 The key limitations of the proposed model are as follows. Firstly, the properties of the
606 walking human SDOF model are identified for free walking and do not consider the effects
607 of the gait parameters such as walking speed and stride length. Secondly, other mechanisms
608 of human-structure and human-human interactions such as synchronisation and lock-in are
609 not considered in this model. Thirdly, the effects of stationary (not moving) people were
610 not considered in this paper. Finally, autonomous simulation of the human-environment
611 interaction is not included in the model.

612 The application of the proposed interaction-based VSA method to experimental data, from
613 six vibration monitoring exercises on two full-scale footbridge structures under different
614 walking traffic, demonstrated the superior performance of the new methodology. The
615 interaction-based VSA method, together with a suitable calibration of human parameters,
616 predicted the occupied structure modal frequency and damping ratio with less than 0.1%
617 and 1% error, respectively. When compared with experimentally measured responses, the
618 new method regularly overestimates the responses by only 5-10%. This is significantly less
619 than 200-500% overestimation obtained when following popular international design
620 guidelines that do not feature the HSI.

621 The method is not suitable for hand-based calculations, which is how VSA is traditionally
622 done. However, if coded and incorporated into a user-friendly software (e.g. with a
623 graphical user interface), it can be used effortlessly in everyday civil engineering practice.
624 Commonly required information for vibration serviceability assessment, such as mode
625 shapes and modal properties of the structure, is provided typically by FEM software or field
626 measurements that involve hardware. This fully computerised approach to VSE can be
627 carried out on a standard PC configuration within minutes.

628 **Acknowledgements**

629 The authors acknowledge the financial support, which came from the University of
630 Sheffield doctoral scholarship for Dr Shahabpoor and the UK Engineering and Physical
631 Sciences Research Council (EPSRC) for the following research grants:

- 632 • Platform Grant EP/G061130/2 (Dynamic performance of large civil engineering
633 structures: an integrated approach to management, design and assessment);
- 634 • Standard Grant EP/I029567/1 (Synchronization in dynamic loading due to multiple
635 pedestrians and occupants of vibration-sensitive structures); and
- 636 • Frontier Engineering Grant EP/K03877X/1 (Modelling complex and partially
637 identified engineering problems: Application to the individualized multiscale
638 simulation of the musculoskeletal system).

639 The authors also acknowledge the contribution of Dr Stana Zivanovic for carrying out the
640 experiments on the Podgorica footbridge.

641

642 **References**

- 643 [1] Racic V, Pavic A, Brownjohn JMW. Experimental identification and analytical
644 modelling of human walking forces: Literature review. *Journal of Sound Vibration*, 2009;
645 326(1–2), 1–49.
- 646 [2] The International Federation for Structural Concrete (FIB). Guidelines for the design of
647 footbridges, 2005.
- 648 [3] International Organization for Standardization (ISO). Bases for design of structures:
649 Serviceability of buildings and walkways against vibrations, ISO 10137:2007, 2007;
650 Geneva.
- 651 [4] Technical Department for Transport, Roads and Bridges Engineering and Road
652 Safety/French Association of Civil Engineering (SETRA/AFGC). Footbridges:
653 Assessment of vibrational behavior of footbridges under pedestrian loading. Technical
654 Guide 0611, 2006, Paris.
- 655 [5] British Standards Institution (BSI). UK national annex to Eurocode 1: Actions on
656 structures. Part 2: Traffic loads on bridges, NA to BS EN 1991-2:2003, 2008; London.
- 657 [6] Racic V, Brownjohn JMW. Stochastic model of near-periodic vertical loads due to
658 humans walking. *Advanced Engineering Informatics*, 2011; 25: 259–75.
- 659 [7] Zivanovic S, Pavic A, Reynolds P. Probability-based prediction of multi-mode
660 vibration response to walking excitation. *Engineering Structures*, 2007; 29(6): 942–54.
- 661 [8] Zivanovic S, Pavic A. Probabilistic modelling of walking excitation for building floors.
662 *Journal of Performance of Constructed Facilities*, 2009; 23(3): 132 – 43.
- 663 [9] Piccardo G, Tubino F. Equivalent spectral model and maximum dynamic response for
664 the serviceability analysis of footbridges. *Engineering Structures*, 2012; 40(7): 445–56.

- 665 [10] Krenk S. Dynamic response to pedestrian loads with statistical frequency distribution.
666 ASCE Journal of Engineering Mechanics, 2012; 138(10): 1275–81.
- 667 [11] Caprani CC, Keogh J, Archbold P, Fanning P. Enhancement factors for the vertical
668 response of footbridges subjected to stochastic crowd loading. Computer and Structures,
669 2012; 102–103: 87–96.
- 670 [12] Caprani CC. Application of the pseudo-excitation method to assessment of walking
671 variability on footbridge vibration. Computers and Structures, 2014; 132: 43–54.
- 672 [13] Zivanovic S, Diaz IM, Pavic A. Influence of walking and standing crowds on structural
673 dynamic properties. Proceeding of Conference & Exposition on Structural Dynamics
674 (IMAC XXVII), 2009.
- 675 [14] Zivanovic S, Pavic A, Ingolfsson ET. Modelling spatially unrestricted pedestrian
676 traffic on footbridges. Journal of Structural Engineering, 2010; 136(10): 1296 – 308.
- 677 [15] Shahabpoor E, Pavic A. Comparative evaluation of current pedestrian traffic models
678 on structures. Conference Proceedings of the Society for Experimental Mechanics Series,
679 2012; 26: 41-52.
- 680 [16] IStructE/DCLG/DCMS Joint Working Group. Dynamic Performance Requirements
681 for Permanent Grandstands: Recommendations for Management Design and Assessment,
682 Institution of Structural Engineers, London, 2008.
- 683 [17] Dougill JW, Wright JR, Parkhouse JG, Harrison RE. Human-structure interaction
684 during rhythmic bobbing, The Structural Engineer, 2006; 22: 32–39.
- 685 [18] Pavic A, Reynolds P. Experimental verification of novel 3DOF model for grandstand
686 crowd-structure dynamic interaction. The proceeding of 26th International Modal Analysis
687 Conference (IMAC XXVI), 2008.

- 688 [19] Jones CA, Pavic A, Reynolds P, Harrison RE. Verification of equivalent mass–
689 spring–damper models for crowd–structure vibration response prediction. Canadian
690 Journal of Civil Engineering; 2011; 38: 1122–35.
- 691 [20] Shahabpoor E, Pavic A, Racic V. Identification of mass–spring–damper model of
692 walking humans. Structures 2016; 5: 233–46.
- 693 [21] Shahabpoor E, Pavic A, Racic V. Using MSD Model to Simulate Human-Structure
694 Interaction during Walking. Conference Proceedings of the Society for Experimental
695 Mechanics Series, 2013.
- 696 [22] Griffin MJ. Handbook of human vibration, Academic Press, London, 1990.
- 697 [23] Racic V, Brownjohn JMW, Pavic A. Reproduction and application of human bouncing
698 and jumping forces from visual marker data. Journal of Sound and Vibration, 2010; 329:
699 3397-416.
- 700 [24] Cox DR. Principles of Statistical Inference. Cambridge University Press, 1st edition,
701 2006.
- 702 [25] Clough W, Penzien J. Dynamics of structures. 2nd edition, McGraw-Hill, New York,
703 1993; ISBN 0-07-011394-7.
- 704 [26] Frazer RA, Duncan WJ, Collar AR. Elementary Matrices. Cambridge University
705 Press, 1957.
- 706 [27] Zivanovic S. Benchmark footbridge for vibration serviceability assessment under
707 vertical component of pedestrian load. Journal of Structural Engineering, 2012; 138(10):
708 1193 – 202.

- 709 [28] Racic V, Pavic A, Brownjohn JMW. Modern facilities for experimental measurement
710 of dynamic loads induced by humans: a literature review. Shock and Vibration, 2013;
711 20(1): 53-67.
- 712 [29] Devore L. Probability and Statistics for Engineering and the Sciences. 8th edition.
713 BROOKS/COLE; 2011; ISBN-13: 978-0538733526.
- 714 [30] Zivanovic S, Pavic A, Reynolds P. Modal testing and FE model tuning of a lively
715 footbridge structure. Engineering Structures, 2006; 28(6): 857-68.
716 doi:10.1016/j.engstruct.2005.10.012
- 717 [31] SICK Sensor Intelligence. LD-PeCo People Counter: Operating instructions. 2009;
718 Available at: <https://www.sick.com/media/pdf/7/47/247/IM0011247.PDF>. Last accessed:
719 10 June 2015.
- 720 [32] Shahabpoor E, Pavic A, Racic, V, Zivanovic S. Effect of group walking traffic on
721 dynamic properties of pedestrian structures. Journal of Sound and Vibration, 2016; In press,
722 <http://dx.doi.org/10.1016/j.jsv.2016.10.017>
- 723 [33] Cox DR, Hinkley DV. Theoretical Statistics, Chapman & Hall, 1974.
- 724 [34] Kendall MG and Stuart DG. The Advanced Theory of Statistics. Vol 2: Inference and
725 Relationship. 1973, Griffin, London.
- 726 [35] Butz C. Beitrag zur Berechnung fußgängerinduzierte Bruckenschwingungen". PhD
727 Thesis (in German); Shaker Verlag Aachen, 2006; ISBN-10 3-8322-5699-7.

Figures

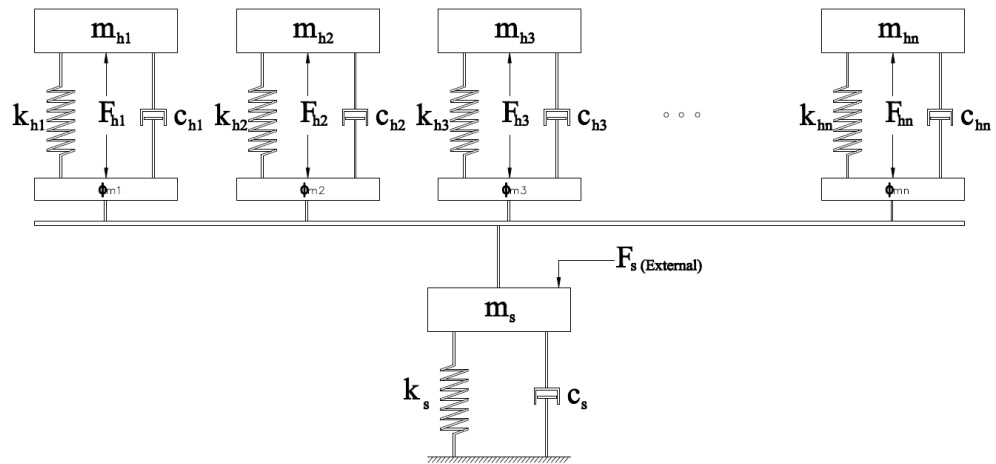


Fig. 1. Mass-spring-damper model of stationary walking traffic-structure system

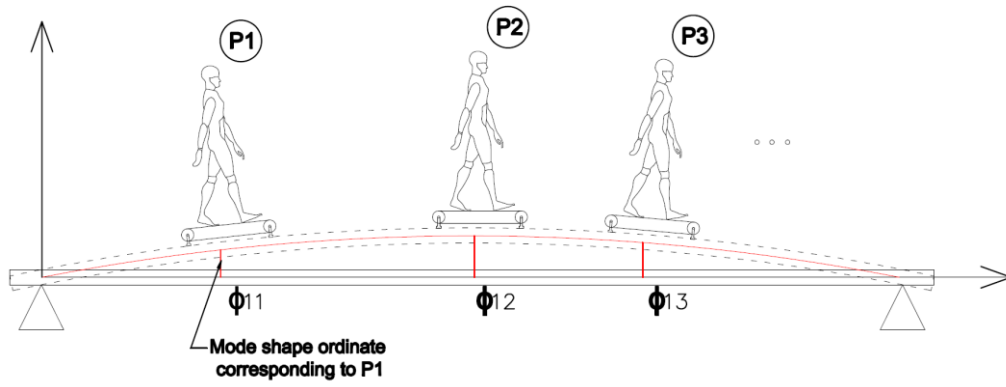


Fig. 2. A conceptual illustration of ‘stationary’ walking people. ϕ represents the ordinate of the mode one shape at the location of each pedestrian.

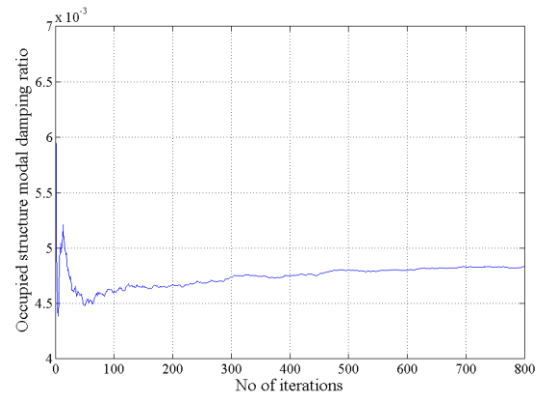
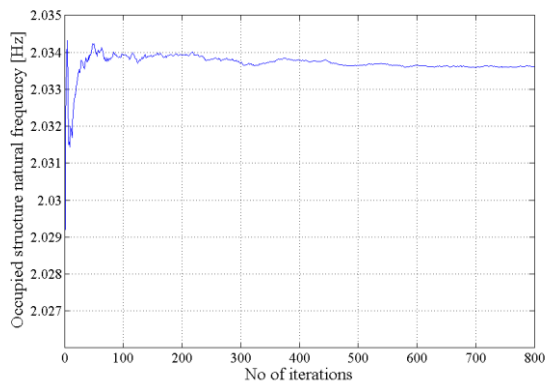
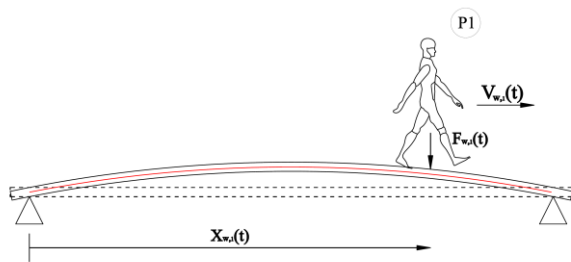
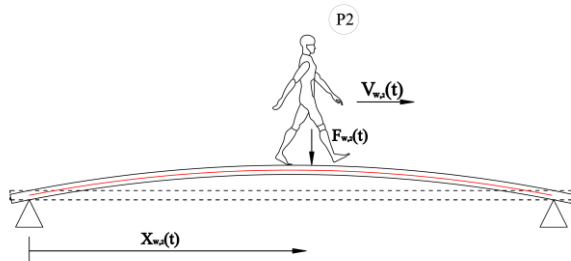


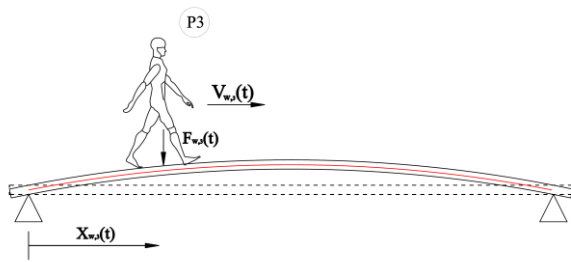
Fig. 3. A typical fluctuation of average occupied structure natural frequency f_{os} and damping ratio ζ_{os}



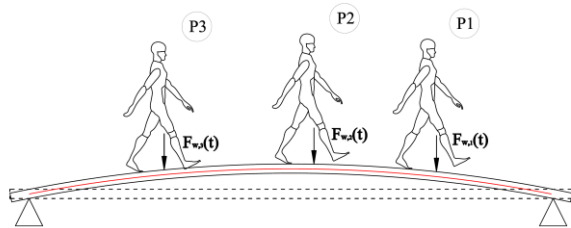
a)



b)



c)



d)

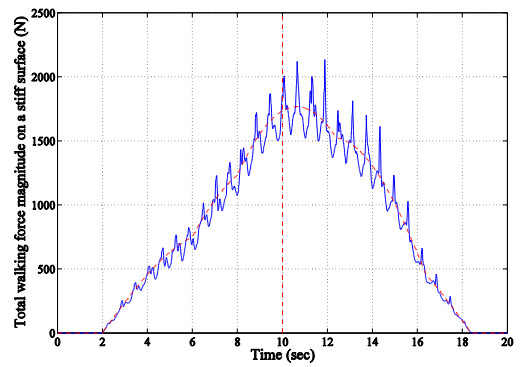
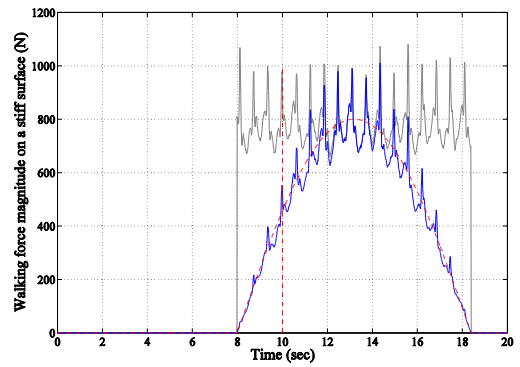
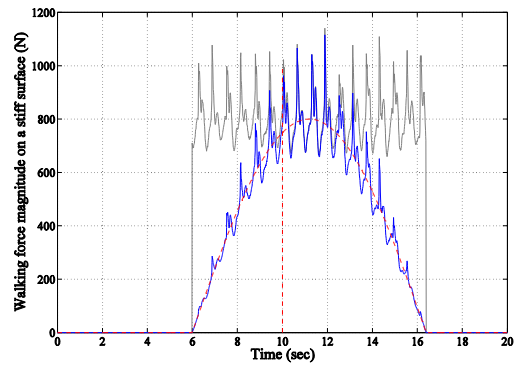
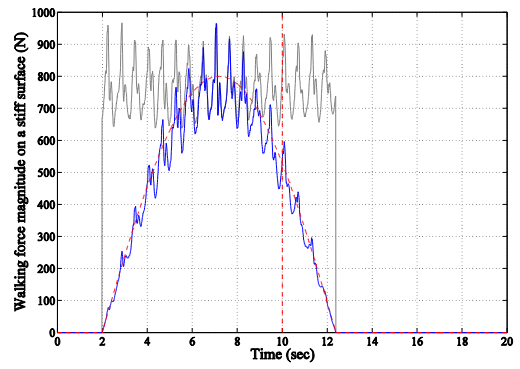
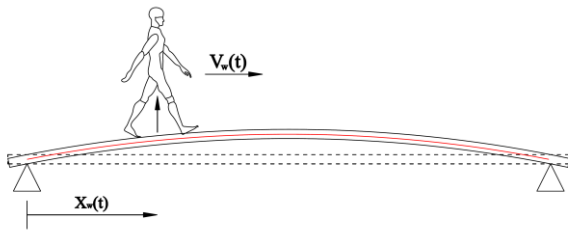
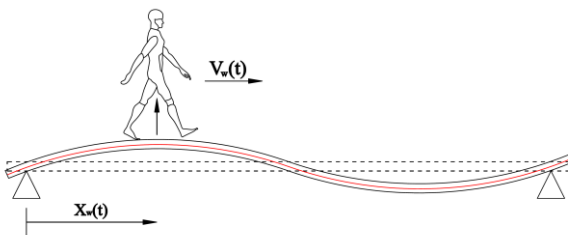
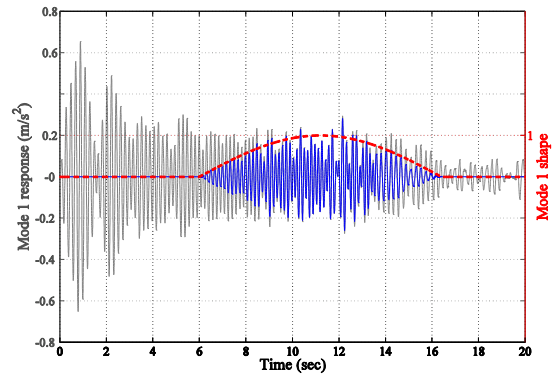


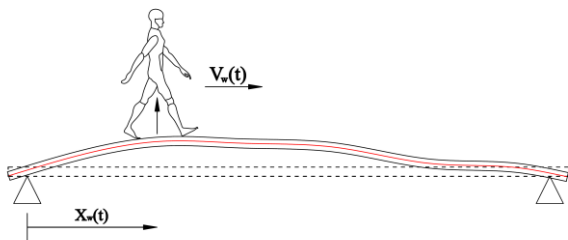
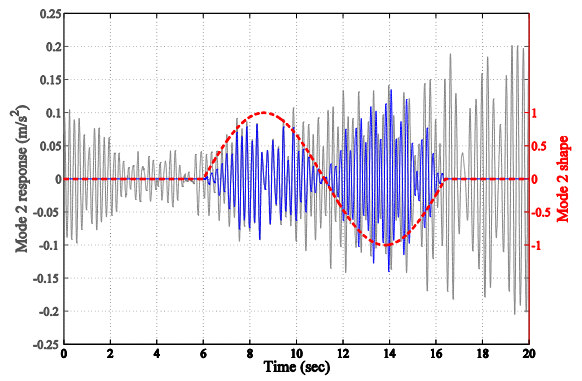
Fig. 4. Superposition of modal walking of three pedestrians (a, b and c) to generate modal force of walking traffic (d) – walking force (grey), modal walking force (blue) and moving average of modal walking force (red)



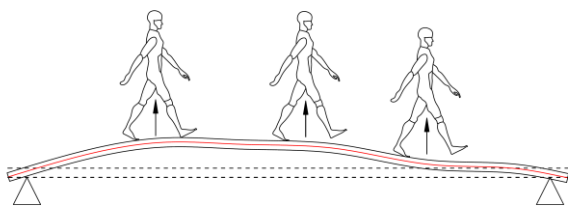
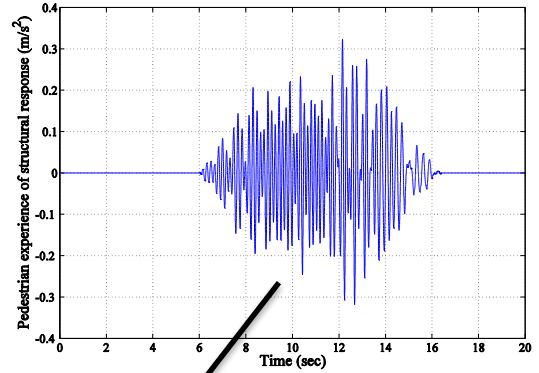
a) Mode 1



b) Mode 2



c) Time-history of pedestrian experience



d) Time-history of traffic experience

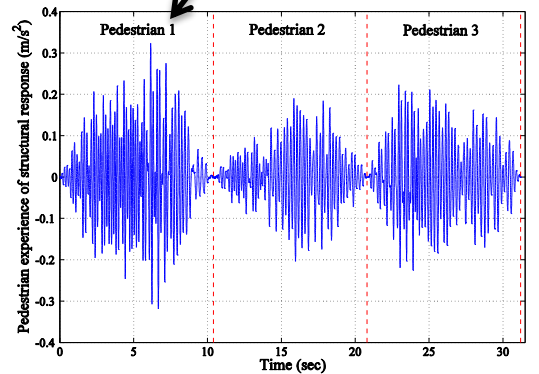
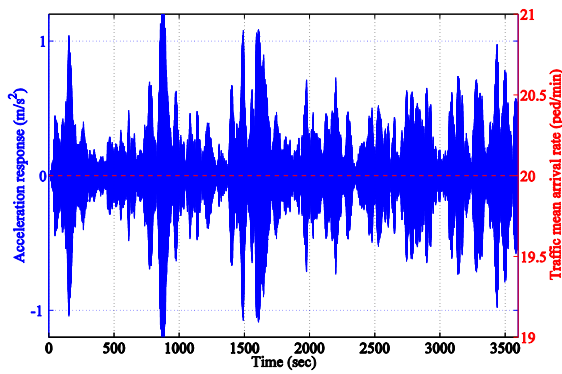
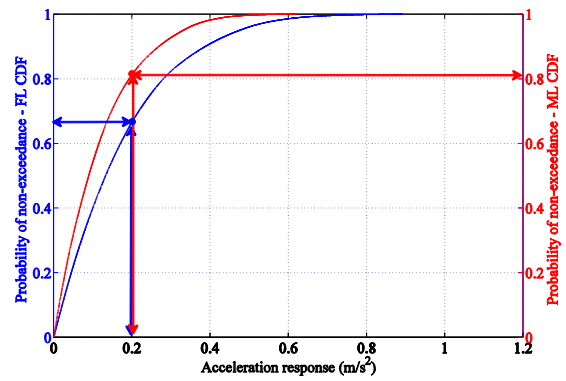


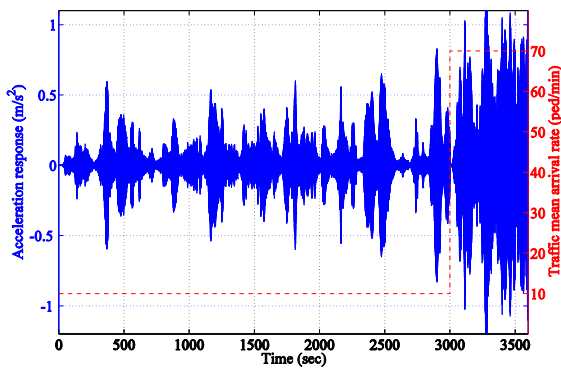
Fig. 5. Time-history of each pedestrian's experience as they walk along the structure



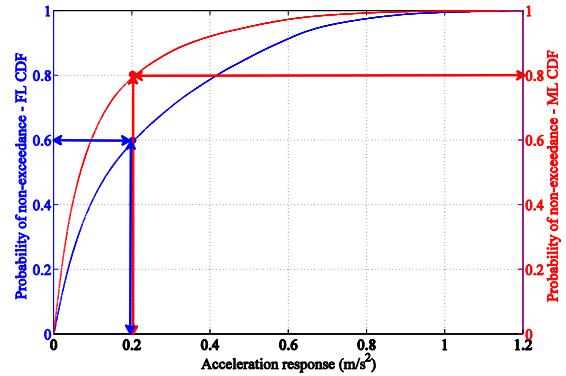
a) Scenario A: Acceleration response and mean arrival rate time-histories



b) Scenario A: Fixed-location (blue) and moving-location (red) CDFs



c) Scenario B: Acceleration response and mean arrival rate time-histories



d) Scenario B: Fixed-location (blue) and moving-location (red) CDFs

Fig. 6. Comparison of FL and ML CDFs

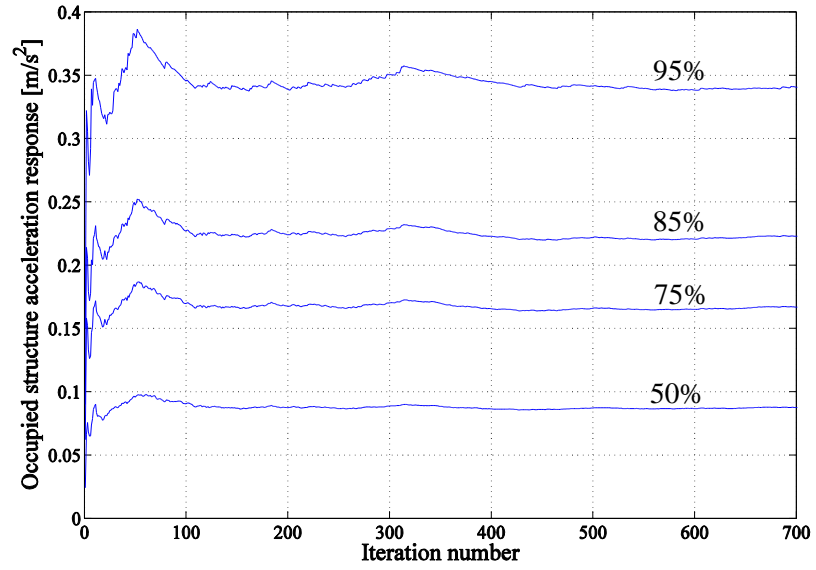
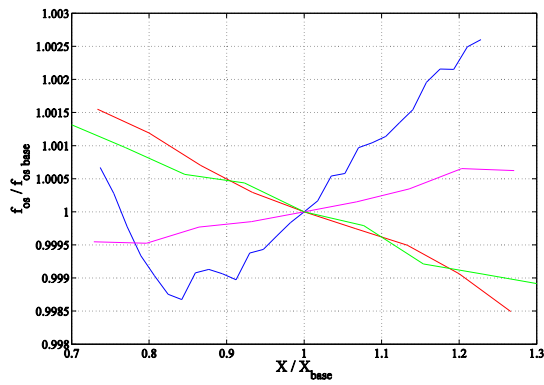
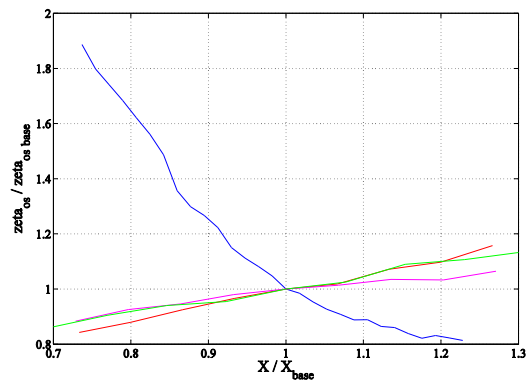


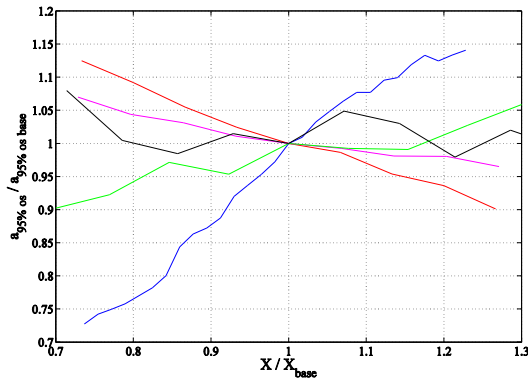
Fig. 7. Typical fluctuation of acceleration response with 95%, 85%, 75% and 50% probability of non-exceedance (from top to bottom)



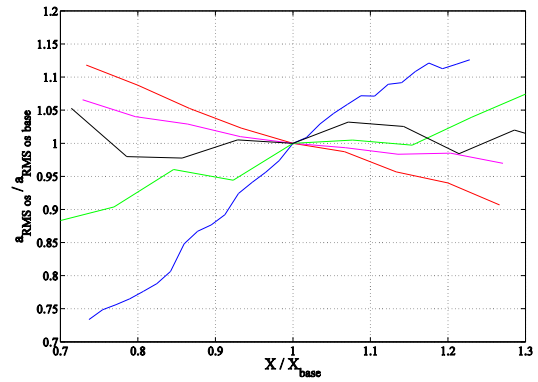
a) Sensitivity of the occupied structure modal frequency f_{os} to input parameters



b) Sensitivity of the occupied structure modal damping ratio ζ_{os} to input parameters



c) Sensitivity of acceleration response with 95% probability of non-exceedance $a_{95\%}$ to input parameters

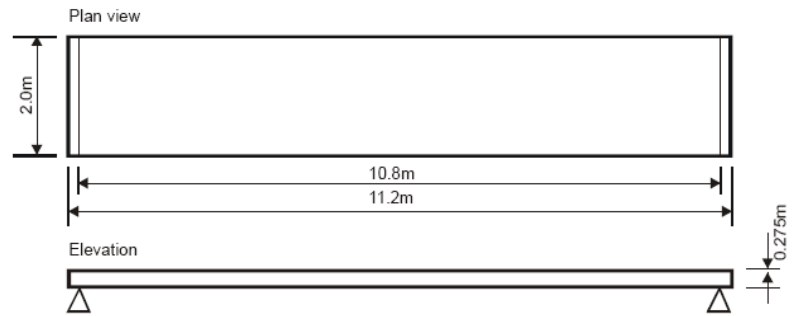


d) Sensitivity of acceleration response RMS a_{rms} to input parameters

Fig. 8. Sensitivity of the interaction-based VSA method outputs f_{os} , ζ_{os} , $a_{95\%}$ and a_{rms} to input parameters (X/X_{base}): mean f_h (blue), m_h (red), ζ_h (pink), arrival rate r_a (green) and walking speed v_w (black)



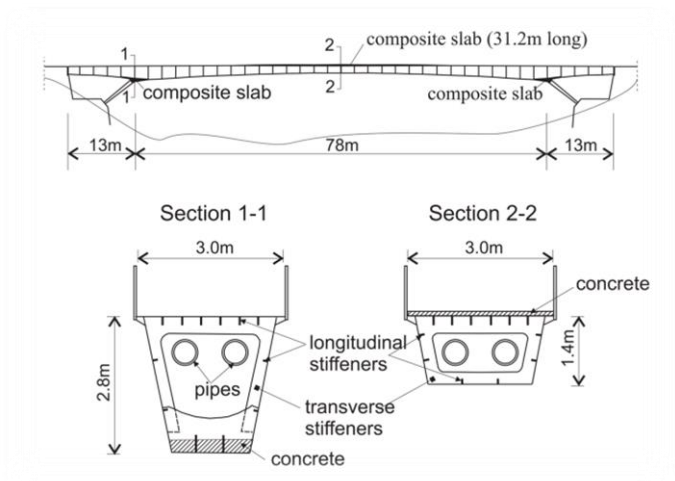
a)



b)

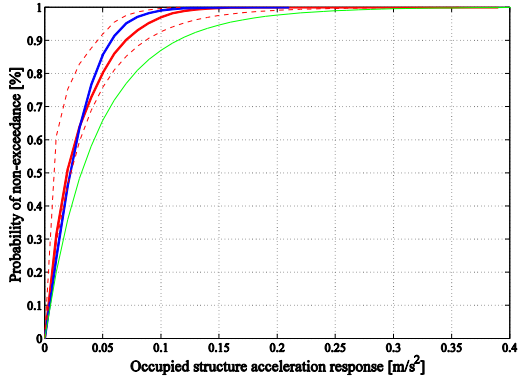


c)

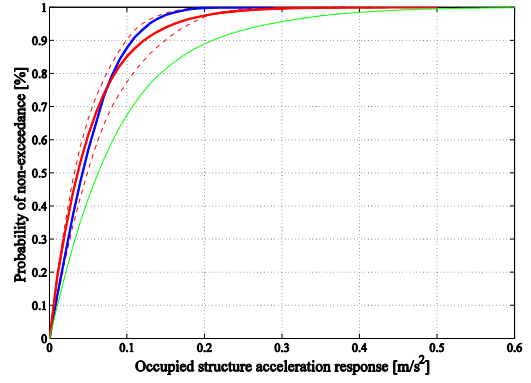


d)

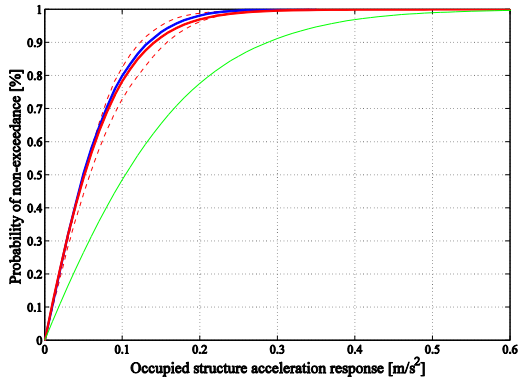
Fig. 9. Photo and schematics of the Sheffield University post-tensioned footbridge (a and b) and Podgorica footbridge (c and d)



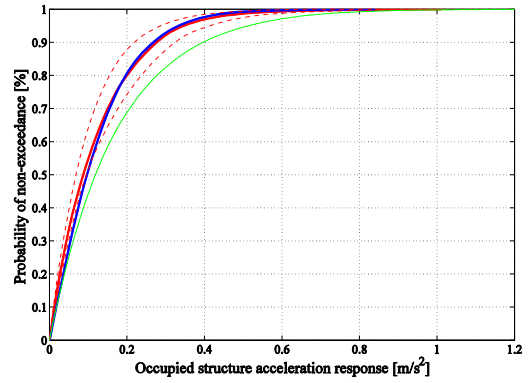
a) Test 1



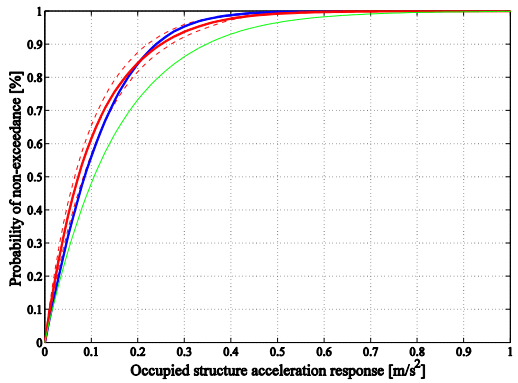
b) Test 2



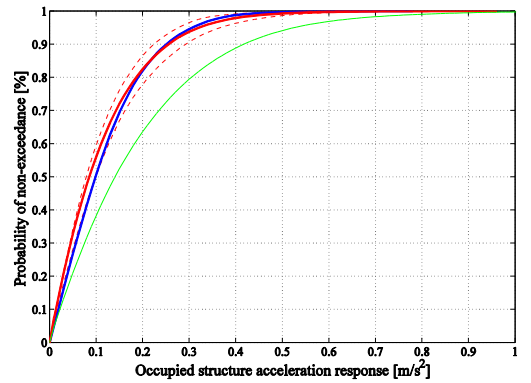
c) Test 3



d) Test 4

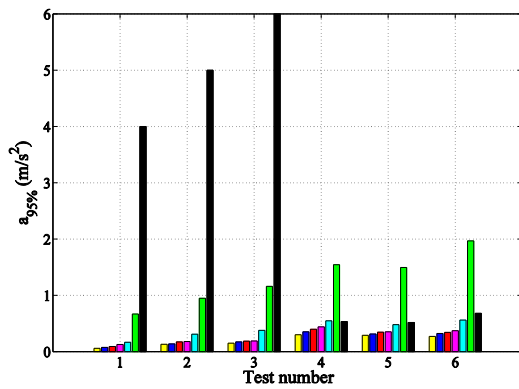


e) Test 5

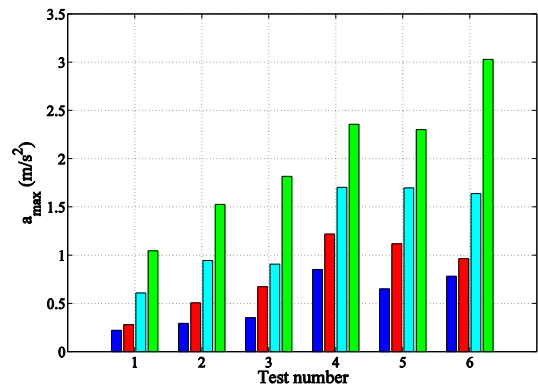


f) Test 6

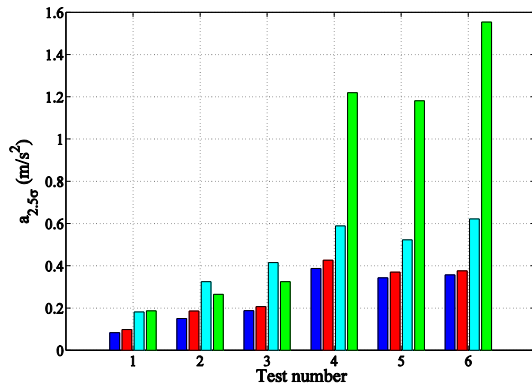
Fig. 10. Comparison of experimental and analytical CDFs. Experimental (blue), confidence interval CDFs (dashed red), the analytical CDF resulted from interaction based VSA method with (red) and without (green) taking into account the HSI effects



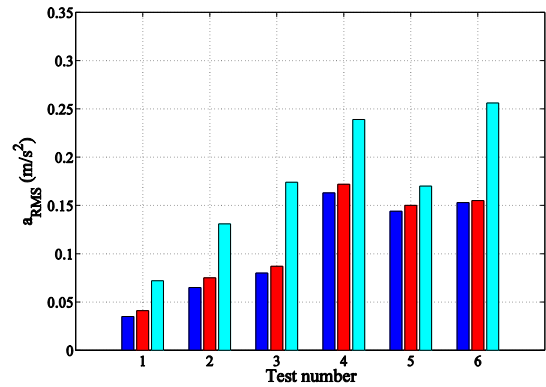
a) Comparison of acceleration response with 95% probability of non-exceedance – in order: experimental (blue), interactive (red), confidence intervals (yellow and magenta), non-interactive (cyan), Setra (green) and Butz (black)



b) Comparison of peak acceleration response - in order: experimental (blue), interactive (red), non-interactive (cyan) and ISO (green)



c) Comparison of acceleration response with $\mu+2.5\sigma$ probability of non-exceedance - in order: experimental (blue), interactive (red), non-interactive (cyan) and UK NA (green)



d) Comparison of acceleration response RMS - in order: experimental (blue), interactive (red), and non-interactive (cyan)

Fig. 11. Comparison of the performance of the interaction-based VSA method (red) with non-interactive (cyan), ISO, UK National Annex, Setra and Butz assessment methods

Tables

Table 1. Traffic statistics of Sheffield and Podgorica footbridges tests

Sheffield footbridge						
<i>Parameter</i>	<i>Unit</i>	<i>Distribution</i>	<i>Test 1</i>	<i>Test 2</i>	<i>Test 3</i>	<i>Average</i>
Number of participants	peds	-	3	6	10	-
Mean arrival rate (r_a)	peds/s	-	0.31	0.63	0.98	-
Mean number of pedestrians on footbridge	peds	-	2.5	4.9	7.86	-
Mean walking speed (v_w)	m/s	Normal	1.41	1.06	1.36	1.28
Variance walking speed (v_w)	m/s	Normal	0.06	0.04	0.29	0.13
Average crossing time (t_c)	s	-	7.7	10.2	7.9	8.4
Average body mass (m_h)	kg	-	70	70	70	70
Podgorica footbridge*						
Mean arrival rate (r_a)	peds/s	Poisson	0.21	0.20	0.35	-
Mean number of pedestrians on footbridge	-	Normal	14.9	15.7	26.1	-
Variance - number of pedestrians on footbridge	-	Normal	4.3	5.9	13.6	-
Mean walking speed (v_w)	m/s	Normal	1.42	1.38	1.38	1.39
Variance walking speed (v_w)	m/s	Normal	0.20	0.21	0.19	0.20
Average crossing time (t_c)	s	-	73.2	75.4	75.4	75
Average body mass (m_h)	kg	-	75	75	75	75

* Values adopted from [26]

Table 2. Statistics of the acceleration response of Sheffield and Podgorica footbridges

<i>Test No.</i>	$a_{peak} (m/s^2)$	$a_{95\%} (m/s^2)$	$a_{2.5\sigma}^* (m/s^2)$	$a_{rms} (m/s^2)$
Sheffield footbridge				
Test 1	0.220	0.074	0.083	0.035
Test 2	0.292	0.133	0.150	0.065
Test 3	0.352	0.172	0.188	0.080
Podgorica footbridge				
Test 4	0.801	0.352	0.387	0.163
Test 5	0.649	0.312	0.343	0.144
Test 6	0.780	0.321	0.357	0.153

* the response amplitude corresponding to 2.5 standard deviation away from mean value of structural response

Table 3. Input parameters of 6 tests used in the interaction-based VSA method

Category	Parameters	Units	Distribution	Sheffield footbridge			Podgorica footbridge		
				Test 1	Test 2	Test 3	Test 4	Test 5	Test 6
Empty Structure modal properties	m_{es}	kg	-		7128			58000	
	f_{es}	Hz	-		4.44			2.04	
	ζ_{es}	%	-		0.6			0.26	
Walking human model parameters	m_h mean	kg	-		70			75	
	f_h mean	Hz	Normal		2.85			2.85	
	f_h variance	Hz	Normal		0.34			0.34	
	ζ_h mean	%	Normal		29.5			29.5	
	ζ_h variance	%	Normal		4.7			4.7	
Traffic parameters	r_a mean	peds/s	Poisson	-	-	-	0.21	0.20	0.35
	v_w mean	m/s	Normal	0.31	0.63	0.98	-	-	-
	v_w variance	m/s	Normal	0.06	0.04	0.29	0.20	0.21	0.19
Walking force	F_w total	N		Recorded with treadmill on a stiff surface					

Table 4. Modal properties of the occupied structures

Test Number	Experimental			Analytical		
	f_{os} (Hz)	ζ_{os} (%)	m_{os} (kg)	f_{os} (Hz)	ζ_{os} (%)	m_{os} (kg)
Sheffield footbridge						
Empty	4.440	0.60	7128	-	-	-
Test 1	4.445	1.10	7183	4.445	1.10	7183
Test 2	4.465	1.65	7238	4.465	1.65	7238
Test 3	4.475	2.30	7311	4.475	2.30	7311
Podgorica footbridge						
Empty	2.04	0.26	58000	-	-	-
Test 4	-**	-**	-**	2.034	0.49	58750
Test 5	-**	-**	-**	2.034	0.49	58750
Test 6	-**	0.67*	-**	2.029	0.65	59300

* Value adopted from [14]

** Value not available

Table 5. Statistical features of the ‘interactive’ and ‘non-interactive’ responses

	Interaction-based VSA method						Non-interactive method			
	a_{peak}	$a_{95\%}$	$a_{95\% \text{ min}}$	$a_{95\% \text{ max}}$	$a_{2.5\sigma}$	a_{rms}	a_{peak}	$a_{95\%}$	$a_{2.5\sigma}$	a_{rms}
Sheffield footbridge										
Test 1	0.280	0.091	0.060	0.125	0.098	0.041	0.607	0.167	0.181	0.072
Test 2	0.505	0.173	0.130	0.180	0.186	0.075	0.944	0.308	0.325	0.131
Test 3	0.673	0.186	0.150	0.190	0.207	0.087	0.907	0.377	0.415	0.174
Podgorica footbridge										
Test 4	1.218	0.397	0.300	0.440	0.426	0.172	1.703	0.548	0.589	0.239
Test 5	1.117	0.345	0.290	0.350	0.370	0.150	1.697	0.480	0.523	0.170
Test 6	0.963	0.341	0.270	0.370	0.376	0.155	1.638	0.560	0.622	0.256